

## Chapter 1

# REDUCED-COMPLEXITY DECENTRALIZED DETECTION OF SPATIALLY NON-CONSTANT PHENOMENA

Gianluigi Ferrari, Marco Martalò, and Marco Sarti

*Wireless Ad-hoc and Sensor Networks (WASN) Laboratory*

*Department of Information Engineering, University of Parma, Parma, Italy*

*E-mail: gianluigi.ferrari@unipr.it, martalo@tlc.unipr.it, marco.sarti@studenti.unipr.it*

**Abstract** In this paper, we study sensor networks with decentralized detection of a *spatially non-constant* phenomenon, whose status *might change* independently from sensor to sensor. In particular, we consider *binary* phenomena characterized by a *fixed* number of status changes (from state “0” to state “1”) across the sensors. This is realistic for sensor networking scenarios where abrupt spatial variations of the phenomenon under observation need to be estimated, e.g., an abrupt temperature increase, as could be the case in the presence of a fire in a specific zone of the monitored surface. In such scenarios, we derive the minimum mean square error (MMSE) fusion algorithm at the access point (AP). The improvement brought by the use of quantization at the sensors is investigated. Finally, we derive simplified (sub-optimum) fusion algorithms at the AP, with a computational complexity lower than that of schemes with MMSE fusion at the AP.

**Keywords:** Decentralized detection, non-constant phenomena, minimum mean square error (MMSE), simplified fusion rule, computational complexity.

## 1. INTRODUCTION

Sensor networks have been an active research field in the last years [1]. In particular, a lot of civilian applications have been developed on the basis of this technology, especially for environmental monitoring [2]. Several frameworks have been proposed for the analysis of sensor networks with a common binary phenomenon under observation [3, 4]. In [5], noisy communication links are modeled as binary symmetric channels (BSCs) and a few techniques, such as the use of multiple observations or selective decentralized detection, are proposed in order to make the system more robust against the noise.

While in [5] the focus is on decentralized detection of a binary phenomenon *common* for all sensors, it is of interest to extend this approach to a scenario where the status of the phenomenon may vary from sensor to sensor. In [6], the authors consider a scenario with a single phenomenon status change (denoted, in the following, as *boundary*) and propose a framework, based on a minimum mean square error (MMSE) detection strategy, to determine the position of the boundary. In [7], under the assumption of proper regularity of the observed boundary, a reduced-complexity MMSE decoder is proposed. In [8], the authors show that an MMSE decoder is unfeasible for large scale sensor networks, due to its computational complexity, and propose a distributed detection strategy based on factor graphs and the sum-product algorithm. Finally, MMSE-based distributed detection schemes have also been investigated in scenarios with a common binary phenomenon under observation and bandwidth constraints [9].

In this paper, we propose an analytical approach to the design of decentralized detection schemes in scenarios with *spatially non-constant* binary phenomena, i.e., phenomena with status (either “0” or “1”) which may vary from sensor to sensor. First, we focus on phenomena with a *single* boundary, i.e., scenarios where there is a single (spatial) position in correspondence to which the phenomenon status changes. Then, we analyze scenarios with a *generic* number of boundaries, i.e., more realistic scenarios where the number of phenomenon status changes may be larger than one. For both these scenarios, we derive the MMSE fusion algorithms<sup>1</sup> at the AP, considering various quantization strategies at the sensors [10]. In order to make our approach practical, we derive simplified fusion algorithms with a computational complexity much lower than that of the MMSE fusion rules. Although heuristic, the simplified fusion algorithms guarantee a *limited* performance loss for sufficiently high values of the sensor SNR.

This paper is structured as follows. In Section 2, we derive MMSE and simplified fusion rules in a scenario where the observed phenomenon is characterized by a single boundary. In Section 3, we extend our framework to the case with a spatially non-constant phenomenon with a generic number of boundaries. In Section 4, numerical results associated with the proposed fusion rules are presented. In Section 5, a simple computational complexity analysis, based on the number of operations required by the derived algorithms, is proposed. Finally, in Section 6 concluding remarks are given.

<sup>1</sup>Note that the proposed MMSE distributed detection schemes are *optimal* in the processing performed at the AP. However, the use of quantization at the sensors makes the overall schemes sub-optimal. Overall optimality holds only for a scenario with no quantization at the sensors.

## 2. PHENOMENA WITH A SINGLE BOUNDARY

### 2.1 MMSE FUSION RULE

Consider a network scenario where  $N$  sensors observe a (spatially) non-constant binary phenomenon characterized by a single status change across the sensors. The phenomenon status can be expressed as  $\mathbf{H} = [H_1, H_2, \dots, H_N]$ , with

$$H_i \triangleq \begin{cases} 0 & \text{if } i < \alpha \\ 1 & \text{if } i \geq \alpha \end{cases} \quad i = 1, \dots, N$$

where the index  $\alpha$  is the position of the *boundary* in correspondence to which the phenomenon status changes (from “0” to “1”). The position of the boundary is modeled as uniformly distributed across the sensors, i.e.,  $P(\alpha = \ell) = 1/N, \ell = 1, \dots, N$ .

The signal observed at the  $i$ -th sensor can be expressed as

$$r_i = c_{E,i} + n_i \quad i = 1, \dots, N$$

where

$$c_{E,i} \triangleq \begin{cases} 0 & \text{if } H_i = 0 \\ s & \text{if } H_i = 1 \end{cases}$$

and  $\{n_i\}$  are additive observation noise samples. Assuming that the noise samples  $\{n_i\}$  are independent with the same Gaussian distribution  $\mathcal{N}(0, \sigma^2)$ , the common signal-to-noise ratio (SNR) at the sensors can be defined as follows:

$$\text{SNR}_{\text{sensor}} = \frac{[\mathbb{E}\{c_{E,i}|H_i = 1\} - \mathbb{E}\{c_{E,i}|H_i = 0\}]^2}{\sigma^2} = \frac{s^2}{\sigma^2}.$$

Each sensor quantizes the observed signal and the value output by the  $i$ -th sensor is denoted as  $d_i \triangleq f_{\text{quant}}(r_i)$ , where the function  $f_{\text{quant}}(\cdot)$  depends on the specific quantization strategy. In the following, we consider (i) binary quantization, (ii) multi-level quantization, and (iii) absence of quantization (i.e., the observations  $\{r_i\}$  are sent to the AP). Based on the messages sent by the sensors, the goal of the AP is to reconstruct, through an MMSE fusion strategy, the status of the distributed binary phenomenon  $\mathbf{H}$ . More precisely, in the considered setting the AP needs to estimate correctly the position of the boundary.

**2.1.1 Binary Quantization.** In this scenario, the  $i$ -th sensor makes a decision comparing its observation  $r_i$  with a threshold value  $\tau_i$ , and computes a local decision  $d_i \in \{0, 1\}$ , i.e.,  $f_{\text{quant}}(r_i) = U(r_i - \tau_i)$ , where  $U(\cdot)$  is the unit step function. In order to optimize the system performance, the thresholds  $\{\tau_i\}$  need to be properly selected. In this paper, a common value  $\tau$  at all sensors is considered. This choice is intuitively motivated by the fact that the sensor

SNR is constant across the sensors. While in a scenario with a common binary phenomenon the relation between  $\tau$  and  $s$  is well known [11], in the presence of a non-constant phenomenon the threshold  $\tau$  needs to be optimized in order to minimize the probability of decision error at the AP. This optimization will be carried out for all the considered scenarios (see the beginning of Section 4 for more details).

The estimated boundary position, denoted as  $\hat{\alpha}$ , can be reasonably chosen as the minimizing value for the mean square error (MSE), i.e.,

$$\hat{\alpha} \triangleq \underset{\tilde{\alpha}=1,\dots,N}{\operatorname{argmin}} \mathbb{E} [|\alpha - \tilde{\alpha}|^2 | \mathbf{d}] \quad (1)$$

where  $\mathbf{d} \triangleq [d_1, d_2, \dots, d_N]$  is the vector of sensors' decisions. The solution of the MMSE problem (1) is well known [12, ch.10]:

$$\hat{\alpha} = \mathbb{E} [\alpha | \mathbf{d}] = \sum_{m=1}^N m P(\alpha = m | \mathbf{d}) \quad (2)$$

where each conditional probability  $P(\alpha = m | \mathbf{d})$  can be expressed, using the Bayes formula and the total probability theorem [13], as

$$P(\alpha = m | \mathbf{d}) = \frac{P(\mathbf{d} | \alpha = m) P(\alpha = m)}{\sum_{\ell=1}^N P(\mathbf{d} | \alpha = \ell) P(\alpha = \ell)}. \quad (3)$$

At this point, one has to calculate the probabilities  $\{P(\mathbf{d} | \alpha = m)\}_m$  in (3). Since the noise samples are independent, conditionally on the value of the boundary position the sensors' decisions are also independent. Therefore, one obtains:

$$P(\mathbf{d} | \alpha = m) = \prod_{k=1}^N P(d_k | \alpha = m) \quad (4)$$

where

$$P(d_k | \alpha = m) = \begin{cases} P \left( \begin{array}{l} d_k=0 \\ n_k > \tau \\ d_k=1 \end{array} \right) & k < m \\ P \left( \begin{array}{l} d_k=0 \\ n_k > \tau - s \\ d_k=1 \end{array} \right) & k \geq m. \end{cases} \quad (5)$$

One should note that expression (5)—and, consequently, the estimated boundary position  $\hat{\alpha}$  in (2)—depends on the particular sequence  $\mathbf{d}$  of sensors' decisions.

The computational complexity required for the evaluation of (2) is very high. For this reason, in the following MMSE-based detection schemes will be applied only in scenarios with a (relatively) small number of sensors. In Section 2.2, we will derive a simplified fusion rule, in order to analyze scenarios with larger numbers of sensors.

**2.1.2 Multi-level Quantization.** Considering  $n_b$  quantization bits, we set the  $2^{n_b} - 1$  quantization thresholds as follows:

$$\frac{s}{2}, \frac{s}{2} \pm \Delta, \frac{s}{2} \pm 2\Delta, \dots, \frac{s}{2} \pm (2^{n_b-1} - 1) \Delta$$

where  $\Delta$  is a system parameter which needs to be properly optimized—more details on its optimization will be provided in Section 4.1. The central threshold corresponds to  $\tau = s/2$ , so that if  $n_b = 1$ , one obtains the scenario with binary quantization [5]. In this case, the sensors' quantized decisions are taken according to the following rule:

$$d_i = \begin{cases} 0 & \text{if } r_i < s/2 - (2^{n_b-1} - 1) \Delta \\ 1 & \text{if } s/2 - (2^{n_b-1} - 1) \Delta \leq r_i < s/2 - (2^{n_b-1} - 2) \Delta \\ \dots & \dots \\ 2^{n_b} - 2 & \text{if } s/2 + (2^{n_b-1} - 3) \Delta \leq r_i < s/2 + (2^{n_b-2} - 1) \Delta \\ 2^{n_b} - 1 & \text{if } r_i > s/2 + (2^{n_b-1} - 1) \Delta. \end{cases} \quad (6)$$

The MMSE fusion algorithm at the AP is similar to that in Section 2.1.1. However, one needs to properly compute the probabilities  $\{P(\mathbf{d}|\alpha = m)\}_m$  in (4). According to (6), expression (5) can be generalized as follows:

$$P(d_k = j|\alpha = m) = \begin{cases} \Phi(\tau - (2^{n_b-1} - 1) \Delta - s \cdot U(m - k + 1)) & \text{if } j = 0 \\ \Phi(\tau - ((2^{n_b-1} - 1) - j) \Delta - s \cdot U(m - k + 1)) \\ -\Phi(\tau - ((2^{n_b-1} - 1) - j + 1) \Delta - s \cdot U(m - k + 1)) & \text{if } j = 1, \dots, 2^{n_b} - 2 \\ 1 - \Phi(\tau + (2^{n_b-1} - 1) \Delta - s \cdot U(m - k + 1)) & \text{if } j = 2^{n_b} - 1 \end{cases} \quad (7)$$

where  $\Phi(x) \triangleq \int_{-\infty}^x \frac{1}{\sqrt{2\pi}} \exp(-y^2/2) dy$ . Obviously, the computational complexity of the fusion algorithm at the AP increases with the use of multi-level quantization. In fact, from (7) one can conclude that  $2^{n_b}$  probability values have to be evaluated—they reduce to  $2^1 = 2$  values in the presence of binary quantization.

**2.1.3 Absence of Quantization.** In this case, the observations at the sensors are not quantized and a local likelihood value, such as the conditional probability density function (PDF) of the observable, is transmitted from each sensor to the AP. Obviously, this is not a realistic scenario, since an infinite bandwidth would be required to transmit a PDF value. However, investigating this case allows to derive useful information about the limiting performance of the considered decentralized detection schemes, since transmission of the PDF of the observables does not entail any information loss at the sensors.

The MMSE estimate of the boundary position can now be written as

$$\hat{\alpha} = \underset{\tilde{\alpha}=1,\dots,N}{\operatorname{argmin}} \mathbb{E} [|\alpha - \tilde{\alpha}|^2 | \mathbf{r}] = \mathbb{E} [\alpha | \mathbf{r}] = \sum_{m=1}^N m P(\alpha = m | \mathbf{r}) \quad (8)$$

where  $\mathbf{r} = [r_1, r_2, \dots, r_N]$  is the vector of the observed signals (rather than the vector of decisions  $\mathbf{d}$  as in (1)). The a posteriori probabilities in (8) can be expressed similarly to (3), i.e.,<sup>2</sup>

$$P(\alpha = m | \mathbf{r}) = \frac{p(\mathbf{r} | \alpha = m) P(\alpha = m)}{\sum_{\ell=1}^N p(\mathbf{r} | \alpha = \ell) P(\alpha = \ell)}$$

where, owing to the independence of the observations,  $p(\mathbf{r} | \alpha = m) = \prod_{i=1}^N p(r_i | \alpha = m)$  and

$$p(r_i | \alpha = m) = \begin{cases} p_{\mathcal{N}}(r_i) & i < m \\ p_{\mathcal{N}}(r_i - s) & i \geq m \end{cases}$$

with  $p_{\mathcal{N}}(n) \triangleq \frac{1}{\sqrt{2\pi\sigma^2}} \exp\left(-\frac{n^2}{2\sigma^2}\right)$ .

## 2.2 SIMPLIFIED FUSION RULE

Since the computational complexity of the MMSE fusion strategy rapidly increases with the number of sensors [6], in this section we derive a simplified low-complexity fusion algorithm. The key idea of this simplified algorithm consists in approximating the MMSE boundary estimate  $\hat{\alpha}$  in (2) (and, similarly, in (8)), which involves a *statistical* average, with a simpler *deterministic* expression. As in Section 2.1, various quantization levels at the sensors are considered. Note that the proposed approach relies on the fact that our goal is to estimate a *single* boundary. However, extensions of this approach to a scenario with multiple boundaries will be considered in Section 3.

**2.2.1 Binary Quantization.** In this case, the boundary position can be estimated as follows:

$$\hat{\alpha} = \underset{1 \leq j \leq N}{\operatorname{argmin}} \left\{ \sum_{i=1}^{j-1} |d_i|^2 + \sum_{i=j}^N |d_i - 1|^2 \right\}. \quad (9)$$

The intuition behind (9) is based on the fact that there is a single boundary: the initial sensors' decisions (from the first to the  $(j-1)$ -th) are compared with "0," whereas the others (from the  $j$ -th to the  $N$ -th) are compared with "1." The

<sup>2</sup>Note that the uppercase  $P$  is used to denote the probability of an event, whereas the lowercase  $p$  is used to denote the PDF of a random variable.

estimated boundary minimizes the simplified cost function  $|\mathbf{d} - \mathbf{d}_j|^2$ , where  $\mathbf{d}_j \triangleq [0, \dots, 0, \underbrace{1}_{j\text{th position}}, \dots, 1]$ , over all possible values of  $j$ .

**2.2.2 Multi-level Quantization.** The approach proposed in Section 2.2.1 can be extended to scenarios with multi-level quantization at the sensors. In particular, we propose the following decision rule at the AP:

$$\hat{\alpha} = \operatorname{argmin}_{1 \leq j \leq N} \left\{ \sum_{i=1}^{j-1} f_1(d_i) + \sum_{i=j}^N f_2(d_i) \right\} \quad (10)$$

where

$$\begin{aligned} f_1(d_i) &\triangleq \min\{|d_i|^2, |d_i - 1|^2, \dots, |d_i - (2^{n_b-1} - 1)|^2\} \\ f_2(d_i) &\triangleq \min\{|d_i - 2^{n_b-1}|^2, |d_i - (2^{n_b-1} + 1)|^2, \dots, |d_i - (2^{n_b} - 1)|^2\}. \end{aligned}$$

The rationale behind (10) is the following. Assuming that the boundary is in the  $j$ -th position, we compare the first  $j - 1$  decisions with the “low” half of the quantization levels (i.e., from 0 to  $2^{n_b-1} - 1$ ), whereas the remaining  $N - j + 1$  decisions are compared with the “high” half of the quantization levels (i.e., from  $2^{n_b-1}$  to  $2^{n_b} - 1$ ). In both groups, the quantization levels closest to the corresponding decisions are selected (through the functions  $f_1$  and  $f_2$ ).

As an aside, we remark that for sufficiently large sensor SNR the estimation strategy in (10) (and, as a special case, in (9)) leads to the same performance obtained with the MMSE fusion strategy.

**2.2.3 Absence of Quantization.** In this scenario, one can use the *a posteriori* probabilities of the two hypotheses at each sensor, conditionally on the observables, to derive the proper objective function. In this case, one can write<sup>3</sup>

$$\hat{\alpha} = \operatorname{argmax}_{1 \leq j \leq N} \left\{ \sum_{i=1}^{j-1} P(H_i = 0 | r_i) + \sum_{i=j}^N P(H_i = 1 | r_i) \right\} \quad (11)$$

where, using Bayes formula and assuming  $P(H_i = 0) = P(H_i = 1)$ ,  $\forall i$ , one has

$$P(H_i = \ell | r_i) = \frac{p(r_i | H_i = \ell)}{p(r_i | H_i = 0) + p(r_i | H_i = 1)} = \frac{p(n_i - \ell \cdot s)}{p(n_i) + p(n_i - s)} \quad \ell = 0, 1.$$

<sup>3</sup>Note that in (11) the “argmax” function is used, instead of the “argmin” function used in (9) and (10), since the objective function needs to be maximized.

### 3. PHENOMENA WITH GENERIC NUMBERS OF BOUNDARIES

In this section, we focus on a network scenario where the status of the phenomenon under observation is characterized by a *generic* number, denoted as  $N_{\text{bs}}$ , of boundaries.<sup>4</sup> This scenario is more realistic than that considered in Section 2, since a generic phenomenon (e.g., the humidity level) could change its status from “0” (e.g., low humidity) to “1” (e.g., high humidity), or vice-versa, in correspondence to more than one sensor. Note that the case with  $N_{\text{bs}} = 1$  corresponds to the previously investigated scenario with a single boundary. The following assumptions are expedient to simplify the derivation of the MMSE detection strategy:

- changes of the phenomenon status are not admitted in correspondence to the first and last sensors, i.e.,  $1 \leq N_{\text{bs}} \leq N - 2$ ;
- the phenomenon status is perfectly known at the first sensor ( $H_1 = 0$ ) and there is no change at the last sensor (i.e.,  $H_N = H_{N-1}$ ).

According to the considered assumptions, the  $N_{\text{bs}}$  boundaries  $\{\alpha_1, \dots, \alpha_{N_{\text{bs}}}\}$  have to satisfy the following relation:

$$2 \leq \alpha_1 < \alpha_2 < \dots < \alpha_{k-1} < \alpha_k < \dots < \alpha_{N_{\text{bs}}} \leq N - 1.$$

Therefore, between 1 and  $\alpha_1 - 1$  the phenomenon status is “0,” between  $\alpha_1$  and  $\alpha_2 - 1$  the phenomenon status is “1,” and so on. In order for the boundary distribution to be realistic, the following condition must necessarily hold:

$$\alpha_{k-1} < \alpha_k \leq (N - 1) - (N_{\text{bs}} - k) = N - N_{\text{bs}} + k - 1 \quad k = 2, \dots, N_{\text{bs}}. \quad (12)$$

Condition (12) formalizes the intuitive idea that the  $k$ -th boundary cannot fall beyond the  $(N - 1 - N_{\text{bs}} + k)$ -th position, in order for the successive (remaining)  $N_{\text{bs}} - k$  boundaries to have admissible positions.

#### 3.1 MMSE FUSION RULE

**3.1.1 Binary Quantization.** Denoting as  $\boldsymbol{\alpha}$  the sequence of boundaries  $(\alpha_1, \dots, \alpha_{N_{\text{bs}}})$ , the MMSE fusion strategy can be determined by directly extending the derivation in Section 2.1.1, obtaining  $\hat{\boldsymbol{\alpha}} = \mathbb{E}[\boldsymbol{\alpha}|\mathbf{d}]$ . On the basis of the assumptions introduced at the beginning of this section, the generic term

<sup>4</sup>We remark that throughout this paper the status of the phenomenon will be supposed independent from sensor to sensor. The existence of *correlations* between sensors would require an extension of the derived algorithms. However, this extension goes beyond the scope of this paper.

of the vector  $\widehat{\boldsymbol{\alpha}}$  can be written as<sup>5</sup>

$$\widehat{\alpha}_k = \mathbb{E}[\alpha_k | \mathbf{d}] = \sum_{\alpha_k=1}^N P(\alpha_k | \mathbf{d}) = \sum_{\alpha_k=k+1}^{N-N_{\text{bs}}+k-1} \alpha_k P(\alpha_k | \mathbf{d}) \quad k = 1, \dots, N_{\text{bs}} \quad (13)$$

where the upper and lower bounds of the sum in the last term are properly modified in order to take into account the constraint (12). The computation of (13) can be carried out by extending (in a multi-dimensional sense) the approach in Section 2.1.1. The probability  $P(\alpha_k | \mathbf{d})$  ( $k = 1, \dots, N_{\text{bs}}$ ) can be obtained by marginalizing the joint probabilities of proper boundaries' sequences. By applying the Bayes formula and the total probability theorem [13], after a few manipulations one obtains

$$P(\boldsymbol{\alpha} | \mathbf{d}) = P(\mathbf{d} | \boldsymbol{\alpha}) P(\boldsymbol{\alpha}) \left[ \sum_{\alpha_1=2}^{N-N_{\text{bs}}} \dots \sum_{\alpha_k=k+1}^{N-N_{\text{bs}}+k-1} \dots \sum_{\alpha_{N_{\text{bs}}}=N_{\text{bs}}+1}^{N-1} P(\mathbf{d} | \boldsymbol{\alpha}) P(\boldsymbol{\alpha}) \right]^{-1}. \quad (14)$$

The first multiplicative term at the right-hand side of (14) can be written as

$$P(\mathbf{d} | \boldsymbol{\alpha}) = \prod_{i=1}^N P(d_i | \boldsymbol{\alpha}) = \prod_{i=1}^{\alpha_1-1} \underbrace{P(d_i | \boldsymbol{\alpha})}_{H_i=0} \prod_{j=\alpha_1}^{\alpha_2-1} \underbrace{P(d_j | \boldsymbol{\alpha})}_{H_j=1} \dots \prod_{q=\alpha_{N_{\text{bs}}}}^N \underbrace{P(d_q | \boldsymbol{\alpha})}_{H_q=0 \text{ or } 1} \quad (15)$$

where we have used the fact that the sensors' decisions are independent. Note that, in the last  $N - \alpha_{N_{\text{bs}}} + 1$  terms,  $H_i = 0$  if  $N_{\text{bs}}$  is *even*, whereas  $H_i = 1$  if  $N_{\text{bs}}$  is *odd*. As in Section 2.1.1, the component conditional probabilities at the right-hand side of (15) can be written as

$$P(d_i | \boldsymbol{\alpha}) = \begin{cases} P \left( \begin{array}{c} d_i = 0 \\ n_i \leq \tau \\ d_i = 1 \end{array} \right) & \text{if } i \in \mathcal{I}_0(\boldsymbol{\alpha}) \\ P \left( \begin{array}{c} d_i = 0 \\ n_i \leq \tau - s \\ d_i = 1 \end{array} \right) & \text{if } i \in \mathcal{I}_1(\boldsymbol{\alpha}) \end{cases} \quad (16)$$

where

$$\mathcal{I}_\ell(\boldsymbol{\alpha}) \triangleq \{\text{indexes } i \text{ such that } H_i = \ell | \boldsymbol{\alpha}\} \quad \ell = 0, 1. \quad (17)$$

The second multiplicative term at the right-hand side of (14), instead, can be written, using the chain rule [13], as

$$P(\boldsymbol{\alpha}) = \prod_{i=1}^{N_{\text{bs}}} P(\alpha_i | \alpha_{i-1}, \dots, \alpha_1) = P(\alpha_1) \prod_{i=2}^{N_{\text{bs}}} P(\alpha_i | \alpha_{i-1}) \quad (18)$$

<sup>5</sup>Note that for ease of notational simplicity, in (13) we use the same notation  $\alpha_k$  to denote both the random variable (in the second term) and its realization (in the third and fourth terms). The same simplified notational approach will be considered in the remainder of Section 3.1. The context should eliminate any ambiguity.

where we have used the fact that the position of the  $i$ -th boundary depends only on the position of the previous  $(i-1)$ -th boundary. Each multiplicative term at the right-hand side of (18) can be written by observing that each boundary is uniformly distributed among the sensors according to the constraints introduced in (13). In particular, by using combinatorics, one obtains

$$\begin{aligned} P(\alpha_1) &= \frac{1}{N - N_{\text{bs}} + 1} \\ P(\alpha_k | \alpha_{k-1}) &= \frac{1}{N - N_{\text{bs}} + k - \alpha_{k-1}} \quad k = 2, \dots, N_{\text{bs}}. \end{aligned}$$

The last term at the right-hand side of (14) (i.e., the denominator) can be easily obtained by observing that it is composed by terms similar to those evaluated in (15) and (18).

Finally, the a posteriori probabilities of the boundaries' positions  $\{P(\alpha_k | \mathbf{d})\}$  ( $k = 1, \dots, N_{\text{bs}}$ ) in (13) can be obtained by proper marginalization of (14):

$$P(\alpha_k | \mathbf{d}) = \sum_{\sim\{\alpha_k\}} P(\alpha_1, \dots, \alpha_{N_{\text{bs}}} | \mathbf{d}) \quad k = 1, \dots, N_{\text{bs}}$$

where the notation  $f(y_i) = \sum_{\sim\{y_j\}} f(y_1, y_2, \dots, y_n)$  ( $i = 1, \dots, n$ ) means that the marginal function  $f(y_i)$  is obtained from the joint function  $f(y_1, y_2, \dots, y_n)$  by summing over all variables  $\{y_j\}$ , with  $j \neq i$  [14].

**3.1.2 Multi-level Quantization.** The derivation of the MMSE fusion algorithm for a scenario with multi-level quantization (with  $n_b$  quantization bits) at the sensors is the same of that provided in Section 3.1.1 for the case with binary quantization. However, as in Section 2.1.2,  $2^{n_b}$  possible values for the decisions at the sensors are admissible (see (6)) and  $2^{n_b}$  probabilities have to be computed (see (7)).

**3.1.3 Absence of Quantization.** Let us finally consider the scenario with no quantization at the sensors, i.e., with the sensors transmitting the PDFs of their observables. As in Section 2.1.3, the estimated boundaries can be written, according to the assumptions outlined at the beginning of Section 3, as

$$\hat{\alpha}_k = \mathbb{E}[\alpha_k | \mathbf{r}] = \sum_{\alpha_k=k+1}^{N-N_{\text{bs}}+k-1} \alpha_k P(\alpha_k | \mathbf{r}) \quad k = 1, \dots, N_{\text{bs}}. \quad (19)$$

The probabilities in (19) can be obtained, as in Section 3.1.1, through proper marginalization of joint conditional probabilities of the following type:

$$P(\boldsymbol{\alpha} | \mathbf{r}) = p(\mathbf{r} | \boldsymbol{\alpha}) P(\boldsymbol{\alpha}) \cdot \left[ \sum_{\alpha_1=2}^{N-N_{\text{bs}}} \dots \sum_{\alpha_i+1}^{N-N_{\text{bs}}+i-1} \dots \sum_{\alpha_{N_{\text{bs}}=\alpha_{N_{\text{bs}}-1}+1}}^{N-1} p(\mathbf{r} | \boldsymbol{\alpha}) P(\boldsymbol{\alpha}) \right]^{-1}.$$

Since sensors' observations are independent, it holds that

$$p(\mathbf{r}|\boldsymbol{\alpha}) = \prod_{i=1}^N p(r_i|\boldsymbol{\alpha})$$

where, similarly to Section 2.1.3,

$$p(r_i|\boldsymbol{\alpha}) = \begin{cases} p_{\mathcal{N}}(r_i) & \text{if } i \in \mathcal{I}_0(\boldsymbol{\alpha}) \\ p_{\mathcal{N}}(r_i - s) & \text{if } i \in \mathcal{I}_1(\boldsymbol{\alpha}) \end{cases}$$

where  $\mathcal{I}_0(\boldsymbol{\alpha})$  and  $\mathcal{I}_1(\boldsymbol{\alpha})$  are defined as in (17).

### 3.2 SIMPLIFIED FUSION RULE

Obviously, the computational complexity of the MMSE distributed detection strategy in scenarios with an arbitrary number of phenomenon boundaries increases more rapidly than in scenarios with a single phenomenon boundary (for more details see Section 5). Therefore, the derivation of simplified fusion algorithms with low complexity (but limited performance loss) is crucial.

A first possible choice is a direct extension of the sub-optimal approach, presented in Section 2.2, for scenarios with a single phenomenon status change. However, this class of simplified fusion algorithms are not efficient in a scenario with multiple boundaries, since the number of comparisons with all possible sequences of boundaries rapidly increases with the number of sensors. Therefore, in the following we introduce another class of reduced-complexity fusion algorithms, which do not make use of these comparisons. As before, depending on the quantization strategy at the sensors, we distinguish three possible scenarios.

**3.2.1 Binary Quantization.** Define the following function:

$$f_{\text{bq}}(k, \mathbf{d}_1^k) \triangleq \sum_{i=1}^k [P(H_i = 0|d_i) - P(H_i = 1|d_i)] \quad k = 1, \dots, N \quad (20)$$

where  $\mathbf{d}_1^k = (d_1, \dots, d_k)$ . The key idea of our approach is the following. The function  $f_{\text{bq}}(k, \mathbf{d}_1^k)$  is monotonically increasing (or decreasing), with respect to  $k$ , while the phenomenon does not change its status. In correspondence to each change of the phenomenon status, the function  $f_{\text{bq}}(k, \mathbf{d}_1^k)$  changes its monotonic behavior. More precisely, a phenomenon variation from "0" to "1" corresponds to a change, trend-wise, from increasing to decreasing; a phenomenon variation from "1" to "0" corresponds to a change, trend-wise, from decreasing to increasing. Therefore, by detecting the changes of the monotonic behavior of  $f_{\text{bq}}$  one can estimate the positions of the boundaries.

The probability  $P(H_i = \ell|d_i)$  ( $\ell = 0, 1; i = 1, \dots, N$ ) in (20) can be written, by applying the Bayes formula and following an approach similar to that in Section 2.2.3, as

$$P(H_i = \ell|d_i) = \frac{P(d_i|H_i = \ell)}{P(d_i|H_i = 0) + P(d_i|H_i = 1)}$$

where we have used the fact that  $P(H_i = 0) = P(H_i = 1)$  and

$$P(d_i|H_i = \ell) = \begin{cases} P(s \cdot \ell + n_i < \tau) = P(n_i < \tau - s \cdot \ell) & \text{if } d_i = 0 \\ P(s \cdot \ell + n_i > \tau) = P(n_i > \tau - s \cdot \ell) & \text{if } d_i = 1. \end{cases}$$

**3.2.2 Multi-level Quantization.** A simplified fusion algorithm for a scenario with multi-level quantization at the sensors can be directly obtained from the one just introduced for the case with binary quantization, with the difference that the probability  $P(d_i|H_i = \ell)$  ( $\ell = 0, 1; i = 1, \dots, N$ ) can assume  $2^{n_b} \geq 2$  values:

$$P(d_i|H_i = \ell) = \begin{cases} P(s \cdot \ell + n_i < \tau - (2^{n_b-1} - 1)\Delta) & \text{if } d_i = 0 \\ P(\tau - (2^{n_b-1} - 1)\Delta \leq s \cdot \ell + n_i < \tau - (2^{n_b-1} - 2)\Delta) & \text{if } d_i = 1 \\ \vdots \\ P(\tau + (2^{n_b-1} - 2)\Delta \leq s \cdot \ell + n_i < \tau + (2^{n_b-1} - 1)\Delta) & \text{if } d_i = 2^{n_b} - 2 \\ P(s \cdot \ell + n_i \geq \tau + (2^{n_b-1} - 1)\Delta) & \text{if } d_i = 2^{n_b} - 1. \end{cases}$$

**3.2.3 Absence of Quantization.** In the absence of quantization at the sensors, one can use the probability  $P(H_i = \ell|r_i)$  ( $\ell = 0, 1; i = 1, \dots, N$ ) and introduce the following function:

$$f_{\text{nq}}(k, \mathbf{r}_1^k) \triangleq \sum_{i=1}^k [P(H_i = 0|r_i) - P(H_i = 1|r_i)] \quad k = 1, \dots, N$$

where  $\mathbf{r}_1^k = (r_1, \dots, r_k)$ . The fusion algorithm at the AP is then the same of that presented in the case with binary quantization, but for the use of  $f_{\text{nq}}$  at the place of  $f_{\text{bq}}$ .

## 4. NUMERICAL RESULTS

We now analyze, through Monte Carlo simulations, the performance of sensor networks using the decentralized detection algorithms previously described. We preliminary denote as  $D(\mathbf{H}, \hat{\mathbf{H}})$  the quadratic distance between the

observed phenomenon  $\mathbf{H}$  and its estimate  $\hat{\mathbf{H}}$ :

$$D(\mathbf{H}, \hat{\mathbf{H}}) \triangleq \left| \langle (\mathbf{H} \oplus \hat{\mathbf{H}}); (\mathbf{H} \oplus \hat{\mathbf{H}}) \rangle \right|^2 \quad (21)$$

where the notation  $\oplus$  stands for bit-by-bit ex-or. Note that  $\hat{\mathbf{H}}$  is the estimated phenomenon, directly derived from the estimated boundaries positions  $\hat{\alpha}$ . We will simply refer to  $D$  as “distance.” We remark that equation (21) reduces to  $D(\mathbf{H}, \hat{\mathbf{H}}) = |\alpha - \hat{\alpha}|^2$  in the case of single-boundary phenomena.

The Monte Carlo simulation results are obtained through the following steps:

1. the number of boundaries and their positions are randomly generated (in the case of a single boundary, only its position is randomly generated);
2. the sensors’ decisions (or the PDFs of the observables, according to the chosen quantization strategy at the sensors) are taken and transmitted to the AP;
3. the AP estimates the boundaries’ positions through either MMSE or simplified fusion algorithms;
4. the distance  $D$  (between the true phenomenon and its estimate) is evaluated on the basis of the estimated sequence of boundaries;
5. steps 1÷4 are repeated a sufficiently large number of times;
6. the average distance  $\bar{D}$  is finally computed.

#### 4.1 SINGLE-BOUNDARY PHENOMENA

In Figure 1.1, the distance  $\bar{D}$  is shown, as a function of the decision threshold  $\tau$  at the sensors, for three different values of the number  $N$  of sensors: (i) 8, (ii) 16, and (iii) 32. The sensor SNR is set to 0 dB. As expected, the optimum value of  $\tau$ , which will be selected, corresponds to  $s/2$  ( $s = 1$  in the considered simulations). When the number of sensors is small, e.g.,  $N = 8$ , the results in Figure 1.1 show that  $\bar{D}$  depends on  $\tau$  in a limited way, and there is not a well-pronounced minimum. The minimum (in correspondence to  $\tau = 0.5$ ) becomes more pronounced when  $N$  increases—obviously, the larger is the number of sensors, the larger is the distance  $\bar{D}$ , since  $\alpha$  can assume a wider set of values. In all numerical results presented in the following, the threshold  $\tau$  is optimized in order to minimize the probability of decision error.

In Figure 1.2, the distance  $\bar{D}$  is shown, as a function of the sensor SNR, in scenarios with binary quantization at the sensors (dashed lines) and, for comparison, with no quantization (solid lines). Three possible values for the number  $N$  of sensors are considered: (i) 8, (ii) 16, and (iii) 32. As expected, the

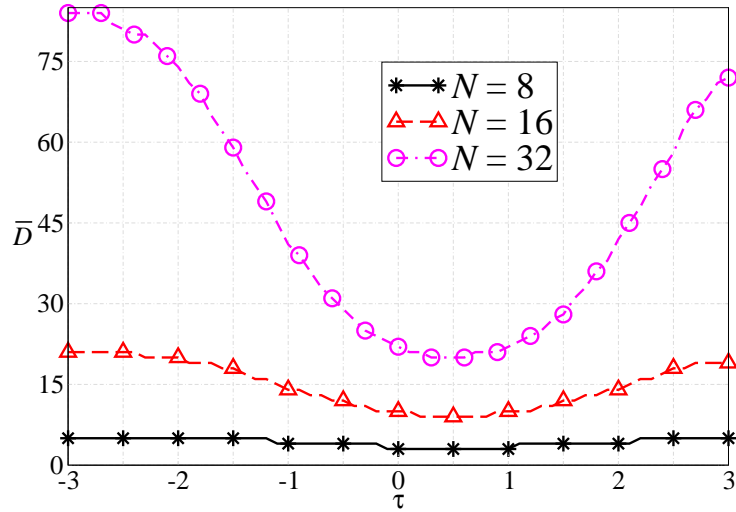


Figure 1.1. Distance, as a function of the decision threshold  $\tau$  at the sensors, in a scenario with a *single boundary* phenomenon, binary quantization, MMSE fusion rule at the AP, and  $\text{SNR}_{\text{sensor}} = 0$  dB. Three possible values of the number  $N$  of sensors are considered: (i) 8, (ii) 16, and (iii) 32.

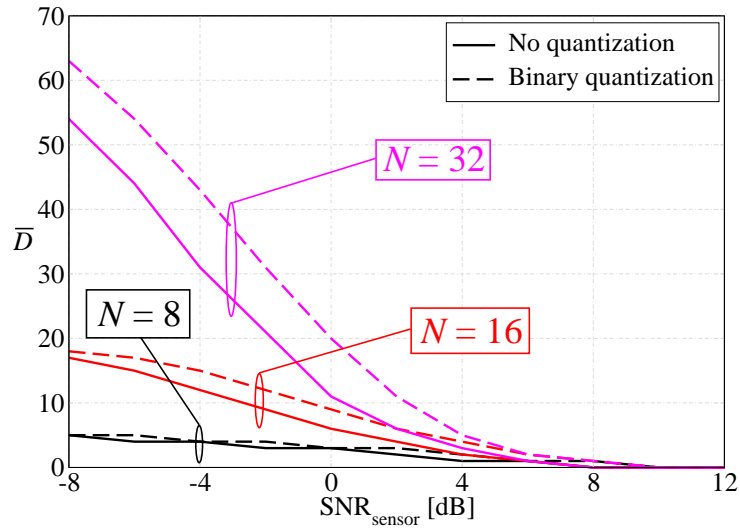


Figure 1.2. Distance, as a function of the sensor SNR, in a scenario with a *single boundary* phenomenon and MMSE fusion rule at the AP. Three possible values for the number  $N$  of sensors are considered: (i) 8, (ii) 16, and (iii) 32. Solid lines correspond to no quantization at the sensors, whereas dashed lines are associated with binary quantization.

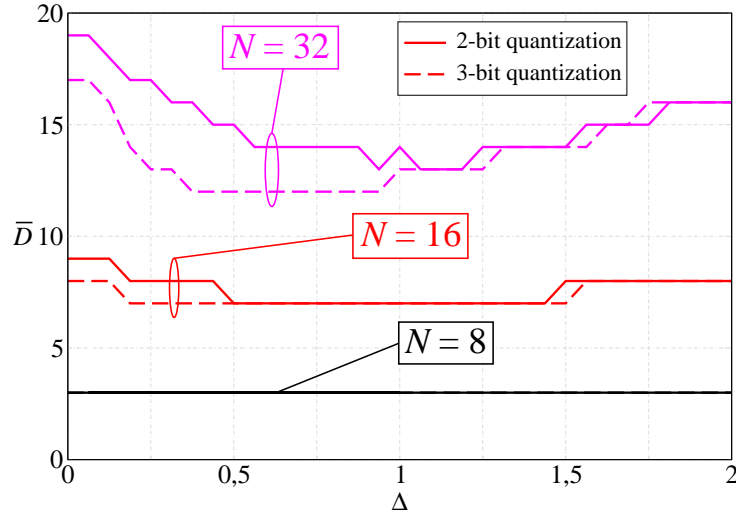


Figure 1.3. Distance, as a function of the quantization parameter  $\Delta$ , in a scenario with a *single boundary* phenomenon, MMSE fusion rule at the AP, multi-level quantization at the sensors, and  $\text{SNR}_{\text{sensor}} = 0$  dB. Three possible values for the number  $N$  of sensors are considered: (i) 8, (ii) 16, and (iii) 32. Solid lines correspond to 2-bit quantization at the sensors, whereas dashed lines are associated with 3-bit quantization.

distance is a decreasing function of the sensor SNR. In fact, when the accuracy of the sensors' observations increases, the decisions sent by the sensors to the AP are more reliable and, consequently, the estimated phenomenon at the AP is closer and closer to the true phenomenon. Note also that the performance degradation incurred by the use of quantization, with respect to the unquantized case, increases for increasing number of sensors.

Let us now turn our attention to a scenario with multi-level quantization at the sensors. First, one needs to optimize the value of  $\Delta$  in (6) for the multi-level quantization scheme. As for the decision threshold  $\tau$ , the optimization is carried out by minimizing the distance  $\bar{D}$ . In Figure 1.3, the distance  $\bar{D}$  is shown, as a function of  $\Delta$ , in a scenario with MMSE fusion strategy at the AP and multi-level quantization at the sensors. The sensor SNR is set to 5 dB. As in Figure 1.1 and Figure 1.2, three possible values for the number  $N$  of sensors are considered: (i) 8, (ii) 16, and (iii) 32. In each case, the performance with 2-bit quantization (solid lines) is compared with that with 3-bit quantization (dashed lines). One can observe that in the case with  $N = 8$  sensors, the performance remains the same regardless of the value of  $\Delta$ . As will be shown later, this is due to the fact that more than one quantization bit at the sensors does not lead to any performance improvement when the number of sensors is too small. On the other hand, the minimum exists in the cases with  $N = 16$  and  $N = 32$ . In the following, for any value of  $N$  the corresponding optimized value of  $\Delta$  will

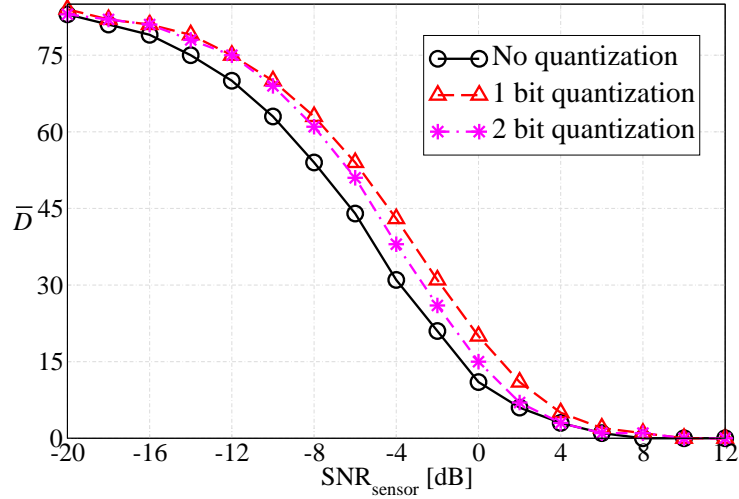


Figure 1.4. Distance, as a function of the sensor SNR, in a scenario with  $N = 32$  sensors, *single boundary* phenomenon, and MMSE fusion rule at the AP. Two possible values for the number of quantization bits at the sensors are considered: (i) 1 and (ii) 2. For comparison, the performance in a scenario with no quantization at the sensors is also shown.

be used. Note that a value of  $\Delta$  slightly larger than 0.5 is practically the best for all considered values of  $N$ .

In Figure 1.4, the distance is shown, as a function of the sensor SNR, in a scenario with  $N = 32$  sensors, MMSE fusion algorithm at the AP, and various quantization levels at the sensors. As expected, the larger is the number of quantization bits, the better is the performance. In fact, a larger amount of information about the observed phenomenon is collected at the sensors and, consequently, the reconstruction of the phenomenon at the AP is more reliable—obviously, the performance in a scenario with no quantization at the sensors represents a lower bound for the distance  $\bar{D}$ . Obviously, there is a price to pay in order to improve the performance through multi-level quantization. In fact, transmission of a larger number of bits leads to higher energy and/or bandwidth consumption.

We now focus on a decentralized detection scheme where the simplified fusion rule derived in Section 2.2 is applied to estimate the boundary position. In Figure 1.5 (a), the distance between the true boundary position and its estimate is shown, as a function of the sensor SNR, in scenarios with no quantization (solid lines) and binary quantization (dashed lines) at the sensors, respectively. Three different values for the number  $N$  of sensors are considered: (i) 8, (ii) 16, and (iii) 32. From the results in Figure 1.5 (a), one can observe that the simplified fusion rule leads to a performance loss with respect to the case with MMSE fusion rule (compare the results in Figure 1.5 (a), for instance, with

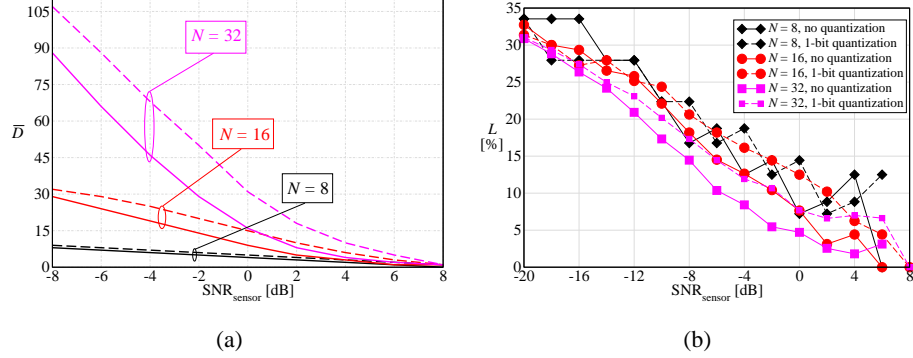


Figure 1.5. Performance, as a function of the sensor SNR, in a scenario with a *single boundary* phenomenon and simplified fusion algorithm at the AP: (a) distance and (b) percentage loss with respect to the MMSE fusion algorithm. Three different values for the number  $N$  of sensors are considered: (i) 8, (ii) 16, and (iii) 32. The performance in the presence of no quantization (solid lines) is compared with that using binary quantization at the sensors (dashed lines).

those in Figure 1.2). However, in the region of interest ( $\text{SNR}_{\text{sensor}} > 0$  dB) the performance with the simplified fusion algorithm is close to that of the MMSE scheme. Moreover, the distance goes to zero with the same trend observed in Figure 1.2 for the MMSE fusion rule.

In order to evaluate the loss incurred by the use of the simplified fusion algorithm, define the following percentage loss:

$$L \triangleq \sqrt{\underbrace{\frac{D^{\text{simp}} - D^{\text{MMSE}}}{D^{\text{MMSE}}}}_{\text{Term}_1} \cdot \underbrace{\frac{D^{\text{simp}} - D^{\text{MMSE}}}{N^2}}_{\text{Term}_2}}. \quad (22)$$

The intuition behind the definition of (22), given by the geometric average of  $\text{Term}_1$  and  $\text{Term}_2$ , is the following.  $\text{Term}_1$  represents the relative loss of the simplified fusion rule with respect to the MMSE fusion rule. However, using only this term could be misleading. In fact, for high sensor SNR, the terms  $D^{\text{simp}}$  and  $D^{\text{MMSE}}$  are much lower than  $N^2$  (the maximum possible quadratic distance). Therefore, even if  $D^{\text{simp}} > D^{\text{MMSE}}$  (for example,  $D^{\text{simp}} = 4$  and  $D^{\text{MMSE}} = 1$  with  $N = 32$ ), both algorithms might perform very well. The introduction of  $\text{Term}_2$  eliminates this ambiguity, since it represents the relative loss (between MMSE and simplified fusion algorithms) with respect to the maximum (quadratic) distance, i.e.,  $N^2$ . In Figure 1.5 (b), the behavior of  $L$  is shown as a function of the sensor SNR. In the region of interest ( $\text{SNR}_{\text{sensor}} \geq 0$  dB), one can observe that  $L$  is lower than 15%, i.e., the proposed simplified fusion algorithm is effective.

In Figure 1.6, we compare directly the performance of MMSE (solid lines) and simplified (dashed lines) fusion algorithms in a scenario with  $N = 16$  sen-

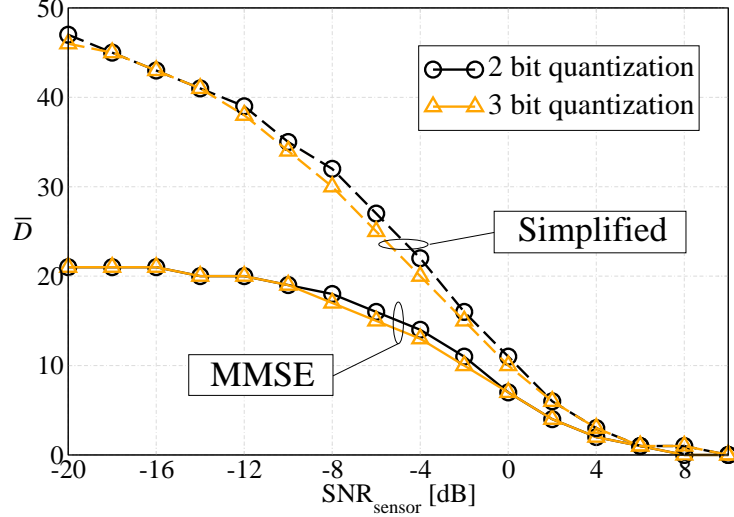


Figure 1.6. Distance, as a function of the sensor SNR, in a scenario with *single boundary* phenomenon and  $N = 16$  sensors. Two possible values of quantization bits at the sensors are considered: (i) 2 bits (circles) and (ii) 3 bits (triangles). The performance with the MMSE fusion rule (solid lines) is compared to that with the simplified fusion rule (dashed lines).

sensors and multi-level quantization. Two possible quantization levels at the sensors are considered: (i) 2-bit (curves with circles) and (ii) 3-bit (curves with triangles). One can observe that, as in Figure 1.4, the performance improves for increasing number of quantization bits. Using a 3-bit quantization level is sufficient to achieve the performance limit corresponding to the absence of quantization—the improvement, with respect to a scenario with 2-bit quantization, is minor.

## 4.2 PHENOMENA WITH MULTIPLE BOUNDARIES

In Figure 1.7, the distance is shown, as a function of the sensor SNR, in a scenario with a multi-boundary phenomenon, for (a)  $N = 8$  sensors and (b)  $N = 32$  sensors. No quantization is considered at the sensors and the performance with the simplified fusion algorithm at the AP is compared directly with that obtained using the MMSE fusion rule. As expected, the distance  $\bar{D}$  reduces to zero for increasing values of the sensor SNR and the performance with the MMSE fusion algorithm is better than that with the simplified fusion algorithm. We recall that the performance with the MMSE fusion rule is evaluated only with  $N = 8$ , since the computational complexity becomes unbearable for values of  $N$  larger than 8 (the simulations are too lengthy).

In order to investigate scenarios with larger numbers of sensors, the use of the reduced-complexity simplified fusion algorithms derived in Section 3.2

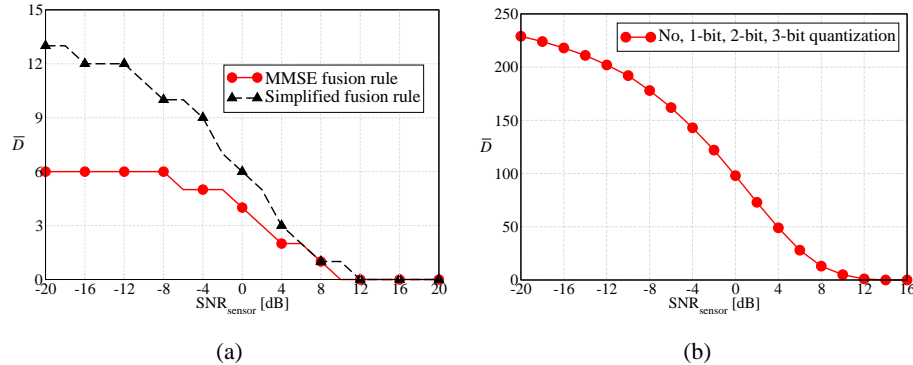


Figure 1.7. Distance, as a function of the sensor SNR, in a scenario with a *multi-boundary* phenomenon, considering (a)  $N = 8$  sensors and absence of quantization (MMSE and simplified fusion algorithms at the AP are considered) is considered and (b)  $N = 32$  and multi-level quantization (only the sub-optimum fusion algorithm at the AP is considered).

is mandatory. In Figure 1.7 (b), the distance is shown, as a function of the sensor SNR, in a scenario with  $N = 32$  sensors and using the simplified fusion algorithm at the AP. Four different quantization scenarios at the sensors are considered: (i) no quantization, (ii) 1-bit quantization, (iii) 2-bit quantization, and (iii) 3-bit quantization. All curves overlap, i.e., the performance does not improve by using more than one quantization bit at the sensors. It remains to be investigated what is the relative loss of the simplified fusion algorithm, with respect to the MMSE fusion algorithm, in scenarios with multi-boundary phenomena. The fact that the quantization strategy at the sensors has little impact suggests that this relative loss might not be negligible.

Finally, we investigate the impact of the number of sensors  $N$  on the system performance. In Figure 1.8, the distance is shown, as a function of the sensor SNR, considering three different values for  $N$ : (i) 8, (ii) 16, and (iii) 32. The simplified fusion algorithm at the AP and 3-bit quantization at the sensors are considered—we remark that similar results hold also for other quantization scenarios. As expected, the smaller is the number of sensors, the smaller is the distance between the observed phenomenon and its estimate. In fact, when the number of sensors increases, the number of phenomenon boundaries increases as well and, consequently, the distance can assume larger values. However, as expected, the distance reduces to zero for sufficiently high values of the sensor SNR.

## 5. COMPUTATIONAL COMPLEXITY

It is now of interest to evaluate the improvement, in terms of computational complexity with respect to the MMSE fusion rule, brought by the use of the

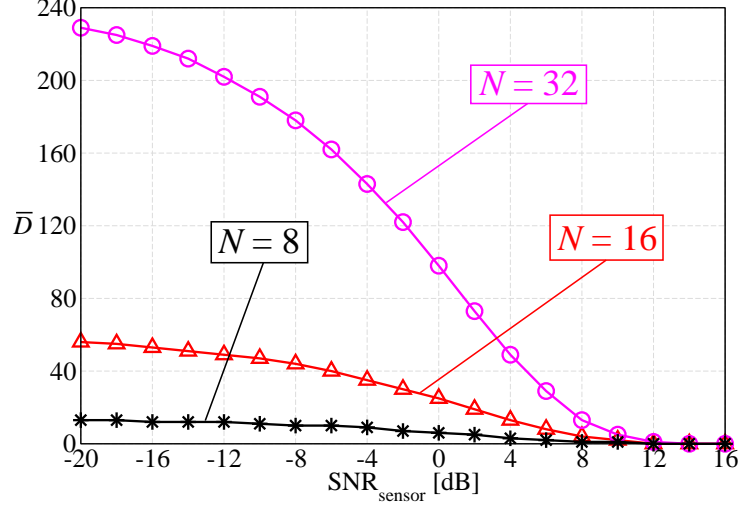


Figure 1.8. Distance, as a function of the sensor SNR, in a scenario with a *multi-boundary* phenomenon, simplified fusion algorithm at the AP, and 3-bit quantization at the sensors. Three different values for the number of sensors  $N$  are considered: (i) 8, (ii) 16, and (iii) 32.

simplified fusion algorithms introduced in Section 2.2 and Section 3.2. As complexity indicators, we choose the numbers of additions and multiplications (referred to as  $N_s$  and  $N_m$ , respectively) required by the considered fusion algorithms.

In a scenario with *single-boundary* phenomena and MMSE fusion rule at the AP, by analyzing (2), (3), and (4), it is possible to show that  $N_s^{\text{opt}} = \Theta(N^2)$  and  $N_m^{\text{opt}} = \Theta(N^3)$ , where the notation  $f(n) = \Theta(g(n))$  means that there exists an  $n_0$  such that for  $n > n_0$ ,  $\exists c_1 \in (0, 1)$ ,  $c_2 > 1$  such that  $c_1 g(n) \leq f(n) \leq c_2 g(n)$  [15]. In a scenario with the simplified fusion algorithm introduced in Section 2.2 (for single-boundary phenomena), instead, by analyzing (9), (10), and (11), it is possible to show that  $N_s^{\text{sub-opt}} = \Theta(N^2)$  and  $N_m^{\text{sub-opt}} = \Theta(N^2)$ . Therefore, one can conclude that the complexity of this simplified fusion algorithm is lower than that of the MMSE fusion algorithm only in terms of the number of multiplications.

Let us now turn our attention to a scenario characterized by phenomena with *multiple boundaries*. By reasoning as in the cases with single-boundary phenomena, the number of operations (in terms of additions and multiplications) required by the MMSE fusion algorithm is  $N_s^{\text{opt}} = \Theta(N^{2N_{\text{bs}}})$  and  $N_m^{\text{opt}} = \Theta(N^{2N_{\text{bs}}+1})$ , respectively—recall that  $N_{\text{bs}}$  is the number of boundaries. As described at the beginning of Section 4, in the considered simulation set-up the number  $N_{\text{bs}}$  of boundaries is chosen randomly between 1 and  $N - 2$ . Therefore, one can assume that the phenomenon is characterized, on average, by

$\frac{N-2}{2} = N/2 - 1$  boundaries. Under this assumption, the computational complexity of the MMSE fusion algorithm would be  $N_s^{\text{opt}} = \Theta(N^{N-2})$  and  $N_m^{\text{opt}} = \Theta(N^{N-1})$ . On the other hand, the reduced-complexity fusion algorithm requires only  $N$  additions, since no multiplication has to be performed. Therefore, the complexity of the proposed simplified fusion algorithm is  $N_m^{\text{sub-opt}} = 0$  and  $N_s^{\text{sub-opt}} = N$ , showing a significant complexity reduction with respect to the MMSE fusion algorithm—this also justifies the non-negligible performance loss for small values of the sensor SNR.

## 6. CONCLUDING REMARKS

In this paper, we have analyzed the problem of decentralized detection of spatially non-constant binary phenomena, i.e., phenomena with statuses characterized by single or multiple boundaries. An analytical framework has been developed to attack this problem, distinguishing between: (i) binary quantization at the sensors, (ii) multi-level quantization, and (iii) no quantization. In all cases, the MMSE fusion algorithm at the AP has been derived and the impacts of relevant network parameters (e.g., the decision threshold at the sensors, the interval of quantization, the sensor SNR, and the number of sensors) have been investigated. Then, we have turned our attention to low-complexity fusion rules. In particular, we have proposed a suboptimal fusion rule, based on a deterministic approximation of the MMSE strategy, in scenarios where the phenomenon has a single boundary. We have further simplified this approach in scenarios with multi-boundary phenomena. Our results show that the performance penalty introduced by the simplified fusion algorithms is asymptotically (for high sensor SNR) negligible. Finally, we have compared the computational complexities of MMSE and simplified fusion algorithms, in terms of required numbers of additions and multiplications. Our results underline that the simplified fusion algorithms allow to reduce the numbers of operations, especially in scenarios with multi-boundary phenomena.

## REFERENCES

- [1] I. Akyildiz, W. Su, Y. Sankarasubramaniam, and E. Cayirci, “A survey on sensor networks,” *IEEE Commun. Mag.*, vol. 40, no. 8, pp. 102–114, August 2002.
- [2] S. N. Simic and S. Sastry, “Distributed environmental monitoring using random sensor networks,” in *Proc. 2-nd Int. Work. on Inform. Processing in Sensor Networks*, Palo Alto, CA, USA, April 2003, pp. 582–592.
- [3] R. Viswanathan and P. K. Varshney, “Distributed detection with multiple sensors—Part I: Fundamentals,” *Proc. IEEE*, vol. 85, no. 1, pp. 54–63,

January 1997.

- [4] I. Y. Hoballah and P. K. Varshney, "An information theoretic approach to the distributed detection problem," *IEEE Trans. Inform. Theory*, vol. 35, no. 5, pp. 988–994, September 1989.
- [5] G. Ferrari and R. Pagliari, "Decentralized binary detection with noisy communication links," *IEEE Trans. Aerosp. Electron. Syst.*, vol. 42, no. 4, pp. 1554–1563, October 2006.
- [6] R. Nowak and U. Mitra, "Boundary estimation in sensor networks: Theory and methods," in *Proc. 2-nd Int. Work. on Inform. Processing in Sensor Networks*, Palo Alto, CA, USA, April 2003.
- [7] R. Nowak, U. Mitra, and R. Willett, "Estimating inhomogeneous fields using wireless sensor networks," *IEEE J. Select. Areas Commun.*, vol. 22, no. 6, pp. 999–1006, August 2004.
- [8] J. Barros and M. Tüchler, "Scalable decoding on factor trees: A practical solution for wireless sensor networks," *IEEE Trans. Commun.*, vol. 54, no. 2, pp. 284–294, February 2006.
- [9] Z.-Q. Luo, "An isotropic universal decentralized estimation scheme for a bandwidth constrained ad hoc sensor network," *IEEE J. Select. Areas Commun.*, vol. 23, no. 4, pp. 735–744, April 2005.
- [10] W. M. Lam and A. R. Reibman, "Design of quantizers for decentralized estimation systems," *IEEE Trans. Commun.*, vol. 41, no. 11, pp. 1602–1605, November 1993.
- [11] W. Shi, T. W. Sun, and R. D. Wesel, "Quasi-convexity and optimal binary fusion for distributed detection with identical sensors in generalized gaussian noise," *IEEE Trans. Inform. Theory*, vol. 47, no. 1, pp. 446–450, January 2001.
- [12] S. M. Kay, *Fundamentals of Statistical Signal Processing, Volume I: Estimation Theory*, Prentice-Hall, Upper Saddle River, NJ, USA, 1993.
- [13] A. Papoulis, *Probability, Random Variables and Stochastic Processes*, McGraw-Hill, New York, NY, USA, 1991.
- [14] F. R. Kschischang, B. J. Frey, and H. A. Loeliger, "Factor graphs and the sum-product algorithm," *IEEE Trans. Inform. Theory*, vol. 47, no. 2, pp. 498–519, February 2001.
- [15] T. H. Cormen, C. E. Leiserson, R. L. Rivest, and C. Stein, *Introduction to Algorithms*, 2nd Edition, MIT Press, Cambridge, MA, USA, 2002.